(26) It must be remembered that for U(IV) ($g_J = \frac{4}{5}$) the spin angular momentum is quantized in the direction *parallel* to the applied magnetic field. This is opposite to the direction in transition metal systems, where orbital angular momentum is partially or totally quenched.[6,20]

(27) (a) W. B. Lewis, J. A. Jackson, J. F. Lemons, and H. Taube, *J. Chem. Phys.*, **36**, 694 (1962); (b) M. P. Eastman, H. G. Hecht, and W. B. Lewis, *ibid.*, **54**, 4141 (1971); (c) W. B. Lewis, S. W. Rabideau, N. H. Krikorian, and W. G. Witteman, *Phys. Rev.*, **170**, 455 (1968); (d) W. Kolbe and N. Edelstein, *Phys. Rev., B*, **4**, 2869 (1971); (e) J. Owen and J. H. M. Thornley, *Rep. Progr. Phys.*, **29**, 675 (1966).

(28) A. Streitwieser, Jr., D. Dempf, G. N. LaMar, D. G. Karraker, and N. Edelstein, *J. Amer. Chem. Soc.*, **93**, 7343 (1971).

(29) (a) G. N. LaMar in ref 20, Chapter 3; (b) R. E. Watson and A. J. Freeman, *Phys. Rev. Lett.*, **6**, 277 (1961).

(30) (a) J. A. Pople and D. L. Beveridge, "Approximate Molecular Orbital Theory," McGraw-Hill, New York, N.Y., 1970, p 80; (b) J. A. Pople, D. L. Beveridge, and P. A. Dobosh, *J. Amer. Chem. Soc.*, **90**, 4201 (1968).

(31) $a_i(CH_2) = -6$ G and $a_i(CH_3) = +23$ G.

(32) (a) R. A. Ogg and J. D. Ray, *Discuss. Faraday. Soc.*, **19**, 237 (1955); (b) R. E. Williams, *J. Inorg. Nucl. Chem.*, **20**, 198 (1961); (c) B. D. James, R. K. Nanda, and M. G. H. Wallbridge, *Inorg. Chem.*, **6**, 1979 (1967); (d) C. H. Bushweller, H. Beall, M. Grace, W. J. Dewkett, and H. S. Bilofsky, *J. Amer. Chem. Soc.*, **93**, 2145 (1971).

(33) (a) R. K. Hertz, H. D. Johnson, II, and S. G. Shore, *Inorg. Chem.*, **12**, 1875 (1973); (b) J. J. Borlin and D. F. Gains, *J. Amer. Chem. Soc.*, **94**, 1367 (1972).

(34) (a) C. H. Bushweller, H. Beall, M. Grace, W. J. Dewkett, and H. S. Bilofsky, *J. Amer. Chem. Soc.*, **93**, 2145 (1971).

(35) T. J. Marks and L. A. Shimp, unpublished observations.

(36) Diamagnetic tetrahydroborates typically have BH_4 resonances in the region $\tau \approx 7.0$–10.0.

(37) For different means to this end see (a) S. R. Tanny, M. Pickering, and C. S. Springer, *J. Amer. Chem. Soc.*, **95**, 6227 (1973); (b) H. S. Gutowsky and H. N. Cheng, *ibid.*, **94**, 5505 (1972); (c) F. A. L. Anet and J. J. Wagner, *ibid.*, **93**, 5266 (1971).

(38) (a) H. S. Gutowsky and C. H. Holm, *J. Chem. Phys.*, **25**, 1228 (1956); (b) A. Allerhand, H. S. Gutowsky, J. Jonas, and R. A. Meinzer, *J. Amer. Chem. Soc.*, **88**, 3185 (1966); (c) C. S. Johnson, Jr., *Advan. Magn. Resonance*, **1**, 33 (1965).

(39) Interestingly, when approaching the slow exchange limit, the line shapes are very insensitive to $\delta\omega$.[38] Thus, resort to superconducting solenoids and other ploys will be of little help in narrowing lines (*e.g.*, to extract coupling constants) in systems which are only slightly exchange broadened.

(40) (a) A. Abragam, "The Principles of Nuclear Magnetism," Oxford University Press, London, 1961, Chapter 8; (b) H. G. Hertz, *Progr. Nucl. Magn. Resonance Spectrosc.*, **3**, 159 (1967); (c) T. C. Farrar and E. D. Becker, "Pulse and Fourier Transform NMR," Academic Press, New York, N.Y., 1971, Chapter 4.

(41) (a) J. P. Kintzinger and J. M. Lehn, *Mol. Phys.*, **54**, 133 (1968); (b) J. H. Noggle and R. E. Schirmer, "The Nuclear Overhauser Effect," Academic Press, New York, N.Y., 1971, p 37.

(42) (a) T. J. Swift in "Chemical Applications of NMR in Paramagentic Molecules," G. N. LaMar, W. D. Horrocks, Jr., and R. H. Holm, Ed., Academic Press, New York, N.Y., 1973, Chapter 2; (b) G. N. LaMar and F. A. Walker, *J. Amer. Chem. Soc.*, **95**, 6950 (1973), and references therein; (c) N. Bloembergen and L. O. Morgan, *J. Chem. Phys.*, **34**, 842 (1961); (d) H. Sternlicht, *ibid.*, **42**, 2250 (1966).

(43) (a) W. DeW. Horrocks, Jr. in ref 20, Chapter 12; (b) J. Reuben and D. Fiat, *J. Chem. Phys.*, **51**, 4918 (1969).

(44) (a) D. Kivelson, *J. Chem. Phys.*, **45**, 1324 (1966); (b) C. P. Poole, Jr., and H. A. Farach, "Relaxation In Magnetic Resonance," Academic Press, New York, N.Y., 1971, Chapter 6.

(45) (a) Reference 44b, Chapter 11; (b) R. Orbach and H. J. Stapleton in "Electron Paramagnetic Resonance," S. Geschwind, Ed., Plenum Press, New York, N.Y., 1972, Chapter 2; (c) C. Y. Huang and M. A. Mostrom, *Phys. Lett. A*, **36**, 46 (1971).

(46) Especially considering the C_5H_5 resonances do not collapse.

(47) At maximum broadness, the resonance is as broad as $(C_5H_5)_3UBH_4$ is at *ca.* −80°. It must be remembered that this line width includes a contribution from spin–spin coupling to the methylene protons of the ethyl group.

(48) This assumes the shifts are transferable from one compound to the other, which is reasonable since the C_5H_5 resonances are so close in frequency (Table II).

(49) (a) H. Kessler, *Angew. Chem., Int. Ed. Engl.*, **9**, 219 (1970). (b) $1/\tau = (kT/h)e^{-\Delta G'/RT}$

(50) (a) G. R. Eaton and W. N. Lipscomb, "NMR Studies of Boron Hydrides and Related Compounds," W. A. Benjamin, New York, N.Y., 1969; (b) R. E. Mesmer and W. L. Jolly, *J. Amer. Chem. Soc.*, **84**, 2039 (1962).

(51) D. S. Marynick and W. N. Lipscomb, *J. Amer. Chem. Soc.*, **95**, 7244 (1973).

(52) Broadline nmr investigations in the solid state offer another possible method of obtaining rate data for very rapid processes. Such studies involving borohydrides are in progress in our laboratories.

(53) (a) D. F. Evans and M. Wyatt, *J. Chem. Soc., Chem. Commun.*, 312 (1972); (b) D. F. Evans and M. Wyatt, *J. Chem. Soc., Dalton Trans.*, 765 (1974).

(54) R. Porter, T. J. Marks, and D. F. Shriver, *J. Amer. Chem. Soc.*, **95**, 3548 (1973), and references therein.

Electronic Structure of Octachlorodimolybdate(II)[1a]

Joe G. Norman, Jr.,* and Harold J. Kolari[1b]

Contribution from the Department of Chemistry, University of Washington, Seattle, Washington 98195.

Received July 25, 1974

Abstract: An all-electron, first-principles SCF-XαSW calculation of the electronic structure of $Mo_2Cl_8^{4-}$ is used to discuss the nature of Mo–Mo and Mo–Cl bonding in this ion and its electronic spectrum. The upper valence region of the energy-level diagram (−0.04 to −0.33 hartree) contains, in order of increasing energy, Mo–Cl bonding, Cl nonbonding, and Mo–Mo σ, π, and δ bonding levels. The δ level is the highest occupied; above it are empty δ^*, two $d_{x^2-y^2}$, π^*, and σ^* antibonding levels. The Mo and Cl character in the upper valence levels is made up almost entirely from 4d and 3p functions, respectively; eight nearly pure Cl 3s levels in the range −0.70 to −0.72 hartree complete the valence region, and no orbitals having large amounts of Mo 5s or 5p character are found. The d-like levels in $Mo_2Cl_8^{4-}$ and hypothetical $MoCl_4^{2-}$ are compared. The σ_n levels postulated by Cotton to lie in the neighborhood of the δ^* level are not found; otherwise the ordering of metal–metal bonding and antibonding levels agrees completely with Cotton's qualitative proposals. Contour maps of the σ, π, and δ wave functions are presented, showing them to be essentially simple overlaps of $4d_{z^2}$, $4d_{xz,yz}$, and $4d_{xy}$ orbitals, respectively, on the metals. The predicted electronic spectrum is in good agreement with the experimental solid-state spectrum of $K_4Mo_2Cl_8 \cdot 2H_2O$. The two well-resolved peaks observed at 18.8 and 31.4 kcm^{-1} are assigned to dipole-allowed $\delta \rightarrow \delta^*$ and $\pi \rightarrow d_{x^2-y^2}$ transitions, respectively. The strong unresolved absorption above 34 kcm^{-1} is believed at least partially due to some combination of Cl $\rightarrow \delta^*$ charge-transfer and $\pi \rightarrow \pi^*$ transitions. The weak band at *ca.* 24 kcm^{-1} is apparently due to one or both of the dipole-forbidden $\pi \rightarrow \delta^*$ and $\delta \rightarrow d_{x^2-y^2}$ transitions. The applicability of the energy-level diagram for $Mo_2Cl_8^{4-}$ to other dimeric complexes of D_{4h} symmetry is discussed.

Metal–metal bond formation has become recognized as one of the most distinctive features in the chemistry of lower oxidation state transition metals. A large number of X-ray structural[2] and Raman spectral[3-5] investigations have shown that the strongest such interactions occur in Cr(II), Mo(II), and Re(III) compounds, with metal–metal distances up to 0.7 Å shorter than expected for single bonds. This agrees with the prediction of Cotton's qualitative molecular orbital treatment[6] that metal–metal bond order should maximize at four (σ-, π-, and δ-type overlaps) for the d^4 electronic configuration. Although this treatment has also successfully rationalized trends in metal–metal distances across a periodic row,[7] and, for a given metal, over a range of oxidation states,[8] several workers have suggested that the proposed ordering of nonbonding and antibonding metal-metal orbitals is not even qualitatively correct in some cases. For example, the validity of the scheme for interpreting electronic spectra[9] of $Mo_2Cl_8^{4-}$ and $Re_2Cl_8^{2-}$, and for correlating observed metal-metal distance with predicted bond order[10] in $Rh_2(O_2CCH_3)_4(H_2O)_2$, has been questioned. Such controversies are possible because, until recently, there has simply been no practical way to carry out reliable quantitative calculations of electronic structure for molecules as large as those under discussion. Extended-Hückel analyses have been presented to both support[11] and challenge[10] the Cotton MO scheme, but this sort of calculation frequently fails for polar molecules to even qualitatively reproduce experimental information about electronic structure and, in view of its ruthless approximations, is not even expected in principle to do so.[12]

The relatively new self-consistent-field, Xα scattered wave (SCF-XαSW) method[13-15] has, especially when the overlapping sphere technique is used,[16] proved capable of accurately describing the electronic structure of quite large inorganic molecules[17-19] in a completely first-principles manner, without expenditure of the large amounts of computer time required for *ab initio* Hartree-Fock calculations. We report here the results of an SCF-XαSW calculation, including analysis of the electronic spectrum, on octachlorodimolybdate(II), $Mo_2Cl_8^{4-}$, perhaps the simplest molecule from the class containing the strongest metal-metal bonds. We believe that this calculation establishes a new, reliable starting point for discussion of the electronic structure of such compounds. A preliminary account of this work has appeared.[20]

Experimental and Calculational Section

Synthesis and Electronic Spectra. $K_4Mo_2Cl_8$ and $K_4Mo_2Cl_8 \cdot 2H_2O$ were prepared by the published method.[21] A Cary 14 instrument was used to record spectra of mineral oil mulls of both solids from 250 to 2100 nm and spectra of solutions in 6 *M* HCl from 220 to 800 nm.

Initial Parameters. The principles of the XαSW method have been thoroughly reviewed[13-16] and compared with those of the Hartree-Fock approach.[22] Coordinates for $Mo_2Cl_8^{4-}$ in atomic units were derived from the average crystallographic bond parameters[23] Mo-Mo = 2.14 Å, Mo-Cl = 2.45 Å, and angle Mo-Mo-Cl = 105°, using the relation 1 bohr = 0.52917 Å and the assumption of full D_{4h} symmetry. The outer sphere was centered at the inversion center of the molecule. The α exchange parameters for Cl and Mo were taken and extrapolated, respectively, from the tabulation of Schwarz;[24] for the extramolecular and intersphere regions, a weighted-average α was used, where the weights were the atomic numbers of electrons (42 for each Mo, 17 for each Cl). Overlapping atomic- and outer-sphere radii were obtained by the nonempirical procedure recently suggested by one of us.[25] Coordinates, α parameters, and sphere radii are summarized in Table I.

Table I. Atomic Coordinates, α Parameters, and Sphere Radii for $Mo_2Cl_8^{4-}$ (Atomic Units)

Region	x	y	z	α	R
Mo_1	0	0	−2.0220	0.70340	2.3811
Mo_2	0	0	2.0220	0.70340	2.3811
Cl_1	4.4722	0	−3.2204	0.72325	2.7125
Cl_2	0	4.4722	−3.2204	0.72325	2.7125
Cl_3	0	−4.4722	−3.2204	0.72325	2.7125
Cl_4	−4.4722	0	−3.2204	0.72325	2.7125
Cl_5	4.4722	0	3.2204	0.72325	2.7125
Cl_6	0	4.4722	3.2204	0.72325	2.7125
Cl_7	0	−4.4722	3.2204	0.72325	2.7125
Cl_8	−4.4722	0	3.2204	0.72325	2.7125
Extramolecular	0	0	0	0.71567	7.7598

SCF Calculation. The initial molecular potential was constructed by superposition of SCF-Xα charge densities for free $Mo^{0.2+}$ and $Cl^{0.55-}$. These initial charges are an arbitrary choice. Throughout the calculation the stabilizing influence of a surrounding crystal lattice on the $Mo_2Cl_8^{4-}$ ion was simulated by adding to the potential that of a "Watson sphere"[26] containing four units of positive charge uniformly distributed over its surface, with radius equal to that of the outer sphere.

Full D_{4h} symmetry was used to factor the secular matrix. The ground-state one-electron eigenvalues converged to ±0.0007 hartree in 25 iterations, using a 9:1 average of the initial and final potentials for a given iteration as the starting potential for the next. Each iteration required about 90 sec of CDC 6400 CP time. Core levels (Mo 1s, 2s, 2p, 3s, 3p, 3d, 4s, 4p and Cl 1s, 2s, 2p) were frozen through the first 18 iterations and thereafter calculated explicitly using only the potential within the sphere surrounding the atom in question.

Excited States. The final ground-state potential was used to search for excited-state levels up to a maximum energy of −0.025 hartree. This potential was then used as the starting point for SCF calculations of the energies of electronic transitions using Slater's transition-state concept.[13] These calculations were done first in spin-restricted form, to obtain a weighted average energy for the singlet and triplet components of a given transition, and then in spin-unrestricted form, to obtain a separate prediction for the triplet. Combination of the two results gives an explicit prediction of the singlet (spin-allowed) transition energy (*e.g.*, for $2b_{2g} \rightarrow 2b_{1u}$, the energy of the $^1A_{1g} \rightarrow {}^1A_{2u}$, rather than $^1A_{1g} \rightarrow {}^3A_{2u}$, process).

Results

The electronic spectrum of $Mo_2Cl_8^{4-}$ in 6 *M* HCl is not reproducible and shows distinct differences from the solid-state spectrum even for freshly prepared solutions. It appears that partial substitution of H_2O for Cl^- occurs immediately upon dissolution,[27] and further reaction takes place more slowly.[28] We therefore compare only the solid-state spectrum with our calculated band positions for $Mo_2Cl_8^{4-}$. The spectrum of solid $K_4Mo_2Cl_8 \cdot 2H_2O$ between 4.8 and 40.0 kcm^{-1} exhibits only two strong bands with well-resolved maxima before the onset of very strong unresolved absorption above 34 kcm^{-1}. These two bands maximize at 18.8 and 31.4 kcm^{-1}, and are of comparable intensity. Except for vibrational overtones, we detect only one other feature between 4.8 and 34 kcm^{-1}, a very weak band at *ca.* 24 kcm^{-1}. Although at the limit of observability in our room-temperature spectrum, this band appears as a distinct, resolved peak in a pellet spectrum of $K_4Mo_2Cl_8$ recorded at 5 °K.[27]

The room-temperature mull spectrum of $K_4Mo_2Cl_8$ is essentially the same as that of the dihydrate, except that the two strong bands are somewhat broader, with a distinct low-energy shoulder appearing on the 31.4 kcm^{-1} maximum. We attribute these small differences to lattice effects, since the crystal structure[23] of $K_4Mo_2Cl_8 \cdot 2H_2O$ shows that the water molecules do not interact significantly with the $Mo_2Cl_8^{4-}$ anion. The conditions of preparation dictate that the dihydrate is inherently a purer material than the anhydrous compound, and hence in the subsequent discussion we use the data for $K_4Mo_2Cl_8 \cdot 2H_2O$ to represent the experimental spectrum of crystal-stabilized $Mo_2Cl_8^{4-}$.

The calculated valence and core one-electron energies and charge distribution for $Mo_2Cl_8^{4-}$ are summarized in Tables II and III, respectively. Levels having more than 20% molybdenum character are diagramed in Figure 1. They are compared there with the d-like levels only from an SCF-XαSW calculation on hypothetical $MoCl_4^{2-}$, performed analogously to that for $Mo_2Cl_8^{4-}$, but in spin-unrestricted form due to the open-shell nature of the monomer. Figures 2-4 are contour maps of the wave functions for the σ, π, and δ Mo-Mo bonding levels, respectively. In Table IV, the calculated energies of all spin- and dipole-allowed

Table II. Ground-State Valence Energy Levels[a] (hartrees) and Charge Distribution[b] for $Mo_2Cl_8^{4-}$

Level	Energy	% 2 Mo	% 8 Cl	Major Mo sph har[c]	Level	Energy	% 2 Mo	% 8 Cl	Major Mo sph har[c]
$4a_{2u}$	−0.038	86	14	d_{z^2}, p_z	$2e_g$	−0.297	6	94	
$5a_{1g}$	−0.042	13	87		$3e_u$	−0.299	2	98	
$5e_g$	−0.048	92	8	$d_{xz,yz}$	$2b_{2u}$	−0.306	23	77	$d_{x^2-y^2}$
$4b_{2u}$	−0.048	76	24	$d_{x^2-y^2}$	$2a_{2u}$	−0.310	2	98	
$4b_{1g}$	−0.070	71	29	$d_{x^2-y^2}$	$3a_{1g}$	−0.312	3	97	
$2b_{1u}$	−0.123	93	7	d_{xy}	$1b_{1u}$	−0.312	7	93	
$2b_{2g}$	−0.155	89	11	d_{xy}	$2e_u$	−0.318	20	80	$d_{xz,yz}$
$5e_u$	−0.204	76	24	$d_{xz,yz}$	$2b_{1g}$	−0.323	25	75	$d_{x^2-y^2}$
$1a_{1u}$	−0.252		100		$1b_{2g}$	−0.325	10	90	
$4a_{1g}$	−0.253	83	17	d_{z^2}, s	$2a_{1g}$	−0.333	28	72	d_{z^2}
$3b_{2u}$	−0.256	0	100		$1b_{2u}$	−0.700	1	99	
$4e_g$	−0.259	1	99		$1e_g$	−0.701	1	99	
$1a_{2g}$	−0.259		100		$1b_{1g}$	−0.706	1	99	
$3e_g$	−0.264	2	98		$1e_u$	−0.708	1	99	
$4e_u$	−0.271	6	94		$1a_{2u}$	−0.711	1	99	
$3a_{2u}$	−0.276	3	97		$1a_{1g}$	−0.718	1	99	
$3b_{1g}$	−0.286	1	99						

[a] The highest occupied level is $2b_{2g}$. [b] % 2Mo and % 8Cl are the percentages of that fraction of charge located within the atomic spheres which reside in the two Mo and eight Cl spheres, respectively. More than 78% of the charge is within the atomic spheres for all levels except $4a_{2u}$ (53%) and $5a_{1g}$ (7%; a diffuse Rydberg-state orbital). [c] The major spherical-harmonic basis functions on Mo contributing to the wave functions for the levels having more than 20% Mo character.

Table III. Ground-State Core Energy Levels (hartrees) for $Mo_2Cl_8^{4-}$

Level	Energy	Level	Energy
Mo 4p	−1.430	Cl 2p	−7.004
Mo 4s	−2.266	Cl 2s	−9.152
Mo 3d	−8.287	Cl 1s	−100.597
Mo 3p	−13.750		
Mo 3s	−16.716		
Mo 2p	−90.951		
Mo 2s	−98.648		
Mo 1s	−709.851		

Table IV. Calculated and Experimental Electronic Spectrum of $Mo_2Cl_8^{4-}$ below 40 kcm^{-1} [a]

Transition	Excited state	Type[b]	Calculated	Experimental[c]
$2b_{2g} \rightarrow 2b_{1u}$	$^1A_{2u}$	$\delta \rightarrow \delta^*$	13.7	18.8
$5e_u \rightarrow 2b_{1u}$	^1E_g	$\pi \rightarrow \delta^*$	23.7	~24
$2b_{2g} \rightarrow 4b_{1g}$	$^1A_{2g}$	$\delta \rightarrow d_{x^2-y^2}$	24.6	
$5e_u \rightarrow 4b_{1g}$	^1E_u	$\pi \rightarrow d_{x^2-y^2}$	34.1	31.4
$4e_g \rightarrow 2b_{1u}$	^1E_u	$Cl \rightarrow \delta^*$	37.5	>34
$3e_g \rightarrow 2b_{1u}$	^1E_u	$Cl \rightarrow \delta^*$	38.6	
$5e_u \rightarrow 5e_g$	$^1A_{2u}$	$\pi \rightarrow \pi^*$	39.4	

[a] Band positions in kcm^{-1}, obtained using the relation 1 hartree = 219.4746 kcm^{-1}. All calculated spin- and dipole-allowed transitions below 40 kcm^{-1}, and the only two spin-allowed, dipole-forbidden transitions which should not be obscured by dipole-allowed bands, are listed. All observed peaks in the range 4.8–40 kcm^{-1} are listed, plus the strong unresolved absorption which begins above 34 kcm^{-1} and apparently maximizes above 40 kcm^{-1}. [b] Largely metal orbitals are denoted σ, π, δ, δ^*, π^*, σ^*, and $d_{x^2-y^2}$ according to their character. Largely ligand orbitals are represented by Cl. [c] From the mineral oil mull spectrum of $K_4Mo_2Cl_8 \cdot 2H_2O$.

electronic transitions below 40 kcm^{-1}, plus the only two spin-allowed, dipole-forbidden transitions that should not be obscured by dipole-allowed bands, are compared with the experimental spectrum of solid $K_4Mo_2Cl_8 \cdot 2H_2O$.

The calculated total energy for $Mo_2Cl_8^{4-}$ is −11627.128 hartrees, and the virial theorem ratio $-2T/V$ is 1.00027, where T and V are the total kinetic and potential energies, respectively. The final intersphere potential energy is −0.2104 hartree. The total charges for each Mo, each Cl, and the extramolecular and the intersphere region are 40.45, 16.81, 1.55, and 7.04 electrons, respectively. Although it might appear that the difference in total energies between one $Mo_2Cl_8^{4-}$ and two $MoCl_4^{2-}$ units is a prediction of the energy change involved in metal-metal bond formation, such a comparison is not in fact valid, because it is necessary to introduce a Watson sphere at an arbitrary position around each ion to achieve a bound solution, and this alters the total energy by an arbitrary and inseparable amount.

Discussion

Inspection of Table II shows that the valence energy levels for $Mo_2Cl_8^{4-}$ can be cleanly separated into several categories; roughly in order of increasing energy, these are as follows. (1) Six nearly pure chlorine 3s levels in the range −0.70 to −0.72 hartree. (2) Four levels having 20-28% Mo character in the range −0.31 to −0.33 hartree, the main contributors to covalent Mo-Cl bonding. (3) Fourteen closely spaced levels having 90-100% Cl character in the range −0.25 to −0.33 hartree, representing nonbonding Cl electrons and contributors to ionic Mo-Cl bonding. (4) Six levels ($4a_{1g}$, $5e_u$, $2b_{2g}$, $2b_{1u}$, $5e_g$, and $4a_{2u}$) having 76-93% Mo character in the range −0.04 to −0.25 hartree, essentially the occupied σ, π, and δ components of the Mo-Mo bond, and their δ^*, π^*, and σ^* antibonding counterparts, respectively. The δ ($2b_{2g}$) and δ^* ($2b_{1u}$) orbitals are the highest occupied and lowest unoccupied, respectively, in the ion. (5) Two unoccupied levels ($4b_{1g}$ and $4b_{2u}$) having 71-76% Mo character in the range −0.05 to −0.07 hartree, antibonding counterparts of Mo-Cl bonding orbitals of the same symmetry ($2b_{1g}$ and $2b_{2u}$) in category 2. (6) A diffuse Rydberg-state orbital ($5a_{1g}$) mainly localized outside the atomic regions at −0.04 hartree, representing essentially a combination of chlorine 4s orbitals.

One thus has a rather classic energy-level diagram for a transition metal complex in the upper valence region—in order of increasing energy, metal-ligand bonding, nonbonding, and metal-ligand antibonding orbitals—except that the last are severely perturbed by being strongly bonding with respect to metal-metal interaction. The perturbations from the case where metal-metal bonding is absent are nicely illustrated by comparison with the d-like orbitals for $MoCl_4^{2-}$ (Figure 1; lower orbitals calculated for $MoCl_4^{2-}$, not shown, are similar to $Mo_2Cl_8^{4-}$). The half-filled, essen-

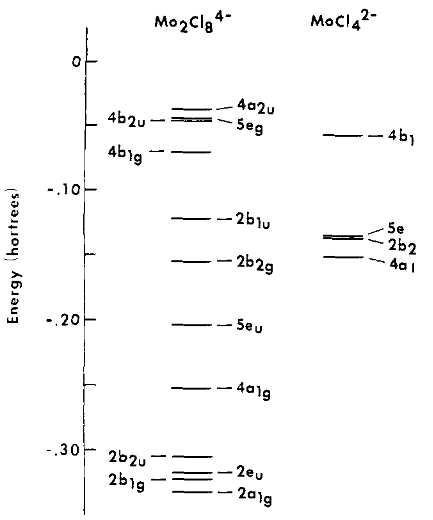

Figure 1. Ground-state valence energy levels for $Mo_2Cl_8^{4-}$ with more than 20% molybdenum character and d-like levels only for $MoCl_4^{2-}$ from an analogous calculation. $2b_{2g}$ and 5e are the highest occupied levels as a whole in the two ions. $Mo_2Cl_8^{4-}$ is closed shell, whereas in $MoCl_4^{2-}$ $4a_1$, $2b_2$, and 5e contain one, one, and two electrons, respectively.

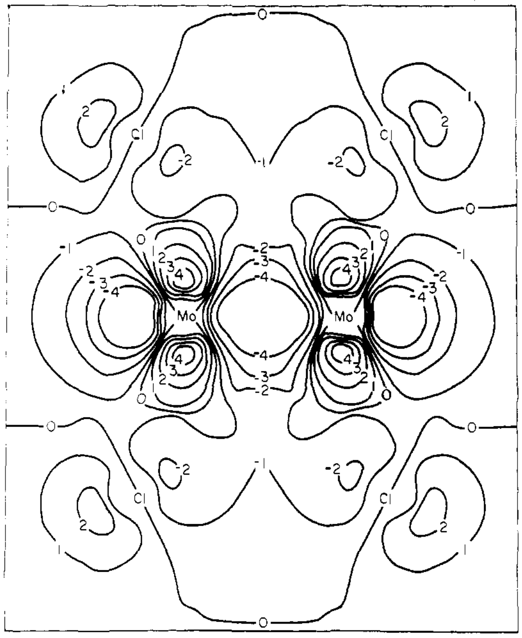

Figure 2. Contour map of the wave function for the $4a_{1g}$ level in the *xz* plane, covering the area 13 × 16 bohrs centered on the origin. The contour values are 0, ±1, ±2, ±3, ±4 = 0, ±0.02, ±0.05, ±0.09, ±0.13, respectively. In this and all subsequent maps, interior contours around Mo and Cl have been omitted for clarity.

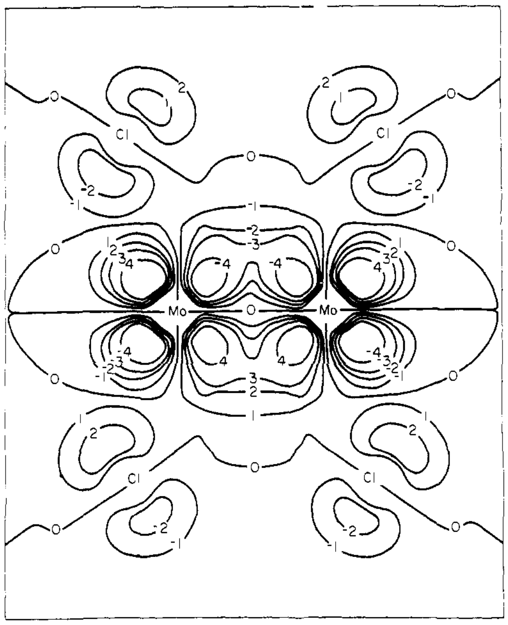

Figure 3. Contour map of one of the two degenerate $5e_u$ wave functions over the same area as Figure 2. The contour values are 0, ±1, ±2, ±3, ±4 = 0, ±0.04, ±0.07, ±0.092, ±0.135, respectively.

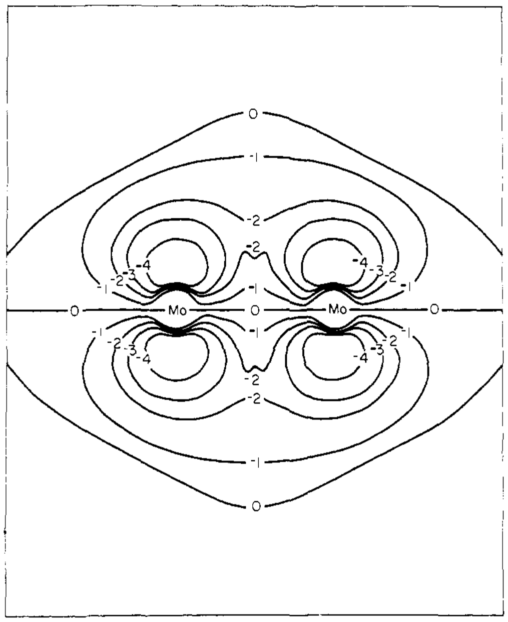

Figure 4. Contour map of the $2b_{2g}$ wave function in the dihedral plane halfway between *xz* and *yz*, covering the area 13 × 16 bohrs centered on the origin. The contour values are 0, ±1, ±2, ±3, ±4 = 0, ±0.01, ±0.04, ±0.075, ±0.14, respectively.

ially $4d_{z^2}$ ($4a_1$), $4d_{xz,yz}$ (5e), and $4d_{xy}$ ($2b_2$) orbitals on the two $MoCl_4^{2-}$ units correlate with the σ ($4a_{1g}$ and $4a_{2u}$), π ($5e_u$ and $5e_g$), and δ ($2b_{2g}$ and $2b_{1u}$) bonding and antibonding metal-metal orbitals in the dimer. The empty, essentially $4d_{x^2-y^2}$ ($4b_1$) orbitals in the $MoCl_4^{2-}$ units remain antibonding Mo-Cl orbitals in the dimer; the symmetric ($4b_{1g}$) and antisymmetric ($4b_{2u}$) combinations split only slightly in energy.

As implied by the above discussion and Table II, the metal contribution to *all* the orbitals of $Mo_2Cl_8^{4-}$ shown in Figure 1, including the lower Mo-Cl bonding levels, is largely made up from 4d rather than 5s or 5p functions. The only levels with any significant non-4d metal character are σ and σ^*, and even here 5s and $5p_z$ functions, respectively, contribute only 10-20%. This has an important consequence for the relation between the present calculations and Cotton's qualitative MO picture.[6] The ordering found for the bonding and antibonding metal-metal orbitals agrees completely with this picture. The only major discrepancy is that we simply do not find the two "σ nonbonding" (σ_n) orbitals of a_{1g} and a_{2u} symmetry postulated by Cotton to lie in the neighborhood of the $2b_{1u}$ level. His postulate was based on the assumption that 5s and $5p_z$ would be important valence orbitals for molybdenum in $Mo_2Cl_8^{4-}$, which our calculation predicts *not* to be the case.

We feel that conclusions previously drawn[6] about metal-metal bond orders *vs.* d^n configuration on the basis of the Cotton diagram, involving population of the σ_n orbitals, may still be largely valid despite the apparent nonexistence of these levels. The reason is that the $4b_{1g}$ and $4b_{2u}$ orbitals which *are* found can fill much the same role as previously assigned to the a_{1g}/a_{2u} set, in the sense that their population should not greatly affect the metal-*metal* bond strength (but should weaken the metal-*ligand* bonds). For example, in $Rh_2(O_2CCH_3)_4(H_2O)_2$, one might expect population of all orbitals in Figure 1 through $4b_{2u}$, retaining a formally triple Rh-Rh bond. There is in fact experimental evidence that the Rh-Rh bond is multiple in nature.[29] Whether the energy-level diagram found for $Mo_2Cl_8^{4-}$ has any general validity for the entire class of basically D_{4h} dimeric complexes remains to be seen. It seems likely that the basic structure of the diagram will be retained, but the metal-ligand antibonding $4b_{1g}$ and $4b_{2u}$ levels may be more sensitive energetically to the exact nature of the metal-ligand bond than are the metal-metal orbitals. Preliminary SCF-XαSW results for $Mo_2(O_2CH)_4$[30] and $Re_2Cl_8^{2-}$[31] seem to confirm this hypothesis. However, $Mo_2Cl_8^{4-}$, $Mo_2(O_2CH)_4$, and $Re_2Cl_8^{2-}$ are all d^4 systems without axial ligands; what changes in the diagram may be wrought by the introduction of additional electrons or ligands can at present only be discussed in a speculative manner.

The σ, π, and δ components of the Mo-Mo bond in $Mo_2Cl_8^{4-}$ are represented pictorially by the wave function contour maps in Figures 2-4. We emphasize that the wave functions mapped there were not constructed as linear combinations of atomic orbitals, nor with the aid of any experimental parameters, but from the direct numerical solution of the molecular one-electron Schrödinger equation by the first-principles scattered wave method.[15] The $4a_{1g}$ σ level is mainly a simple overlap of $4d_{z^2}$ functions on the metals. The outer lobes and equatorial rings of the $4d_{z^2}$ functions are antibonding with respect to Mo-Cl interaction, as shown by the nodes between the Mo and Cl parts of the wave function, but it is interesting that the Mo-Mo bond region interacts weakly with the 3p-like chlorine orbitals in a bonding fashion, as shown by the range of the central -1 contour.[32] The $5e_u$ π orbital shown is essentially a metal-metal $4d_{xz}$ overlap, and similar comments to the above apply to it. Finally, the half of the $2b_{2g}$ δ orbital pictured shows the face-on overlap of metal $4d_{xy}$ functions; it should be borne in mind that an identical picture 90° to the one shown makes up the other half of the function. The relative values of the largest contours enveloping both metal centers show that the strength of the individual bond components decreases in the order $\sigma > \pi > \delta$, as expected and is indicated by the relative σ-σ^*, π-π^*, and δ-δ^* separations on the energy-level diagram—although of course the two degenerate π bonds together are probably stronger than the single σ bond. It is worth noting at this point that Figures 2-4 would be scarcely believable to inorganic chemists of a generation ago. Rigorous, first-principles calculations on heavy metal systems were not at that time believed possible nor was the concept of strong, covalent metal-metal bonding in discrete molecules a familiar one.

Comparison of the predicted electronic spectrum of $Mo_2Cl_8^{4-}$ with the experimental observations for solid $K_4Mo_2Cl_8 \cdot 2H_2O$ reveals a logical assignment of the observed bands to particular one-electron transitions (Table IV). Four regions of absorption are predicted below 40 kcm^{-1}, with the second relatively weaker in intensity because of its dipole-forbidden character. This is exactly what is observed. Our calculations thus support the recent experimental assignment,[9] based on single-crystal polarized spectra, of the 18.8-kcm^{-1} band in $Mo_2Cl_8^{4-}$ to the $\delta \rightarrow \delta^*$ transition. It appears that the weak band at *ca.* 24 kcm^{-1} represents one or both of the dipole-forbidden $\pi \rightarrow \delta^*$ and $\delta \rightarrow d_{x^2-y^2}$ transitions; at present we have no way of predicting which of two transitions allowed only by vibronic mechanisms should be the stronger. We *suggest* that the 31.4-kcm^{-1} band corresponds to a $\pi \rightarrow d_{x^2-y^2}$ transition and that the strong unresolved absorption above 34 kcm^{-1} is at least partially due to charge-transfer ($Cl \rightarrow \delta^*$) or $\pi \rightarrow \pi^*$ transitions or some combination of the two. The agreement between predicted and observed transitions is quite good, considering that the spectral-transition calculations, even in spin-unrestricted form, are inherently more approximate than XαSW calculations of a closed-shell ground-state configuration and that the Watson-sphere technique is a less-than-ideal way of representing the effect of the surrounding crystal lattice in $K_4Mo_2Cl_8 \cdot 2H_2O$ on the $Mo_2Cl_8^{4-}$ anion.

Further SCF-XαSW calculations are in progress or planned on *neutral* dimers containing strong metal-metal bonds, such as molybdenum(II) and rhodium(II) formate, where there is hope of obtaining a direct correlation of predicted ionization energies with experiment. Preliminary SCF-XαSW results for $Re_2Cl_8^{2-}$, together with single-crystal polarized spectra,[31] suggest that the three strong bands found below 40 kcm^{-1} are due to $\delta \rightarrow \delta^*$, $Cl \rightarrow \delta^*$, and $\pi \rightarrow \pi^*$ transitions, in order of increasing energy, as compared to our assignments of the three strong bands in $Mo_2Cl_8^{4-}$ to $\delta \rightarrow \delta^*$, $\pi \rightarrow d_{x^2-y^2}$, and $\pi \rightarrow \pi^*$ or $Cl \rightarrow \delta^*$ transitions.

Acknowledgment. We thank the donors of the Petroleum Research Fund, administered by the American Chemical Society, and the Research Corporation for support. We are grateful to Professors H. B. Gray and R. J. H. Clark for communication of results prior to publication and to E. R. Byrd and E. O. Fey for assistance with some of the spectral measurements.

References and Notes

(1) (a) Presented in part at the 167th National Meeting of the American Chemical Society, Los Angeles, Calif., March 31–April 5, 1974. (b) NSF Predoctoral Trainee, 1973–1974.
(2) F. A. Cotton, J. M. Troup, T. R. Webb, D. H. Williamson, and G. Wilkinson, *J. Amer. Chem. Soc.*, **96**, 3824 (1974), and references therein.
(3) R. J. H. Clark and M. L. Franks, *J. Chem. Soc., Chem. Commun.*, 316 (1974).
(4) A. P. Ketteringham and C. Oldham, *J. Chem. Soc., Dalton Trans.*, 1067 (1973).
(5) J. San Filippo, Jr., and H. J. Sniadoch, *Inorg. Chem.*, **12**, 2326 (1973).
(6) F. A. Cotton, *Accounts Chem. Res.*, **2**, 240 (1969).
(7) F. A. Cotton and J. G. Norman, Jr., *J. Amer. Chem. Soc.*, **94**, 5697 (1972), and references therein.
(8) M. Chisholm, F. A. Cotton, B. A. Frenz, and L. Shive, *J. Chem. Soc., Chem. Commun.*, 480 (1974), and references therein.
(9) C. D. Cowman and H. B. Gray, *J. Amer. Chem. Soc.*, **95**, 8177 (1973).
(10) L. Dubicki and R. L. Martin, *Inorg. Chem.*, **9**, 673 (1970).
(11) F. A. Cotton and C. B. Harris, *Inorg. Chem.*, **6**, 924 (1967).
(12) J. P. Lowe, *J. Amer. Chem. Soc.*, **96**, 3759 (1974).
(13) J. C. Slater and K. H. Johnson, *Phys. Rev. B*, **5**, 844 (1972).
(14) K. H. Johnson, J. G. Norman, Jr., and J. W. D. Connolly in "Computational Methods for Large Molecules and Localized States in Solids," F. Herman, A. D. McLean, and R. K. Nesbit, Ed., Plenum Press, New York, New York, 1972, pp 161–201.
(15) K. H. Johnson, *Advan. Quantum Chem.*, **7**, 143 (1973).
(16) N. Rösch, W. G. Klemperer, and K. H. Johnson, *Chem. Phys. Lett.*, **23**, 149 (1973).
(17) N. Rösch and K. H. Johnson, *Chem. Phys. Lett.*, **24**, 179 (1974).
(18) N. Rösch, R. P. Messmer, and K. H. Johnson, *J. Amer. Chem. Soc.*, **96**, 3855 (1974).
(19) J. G. Norman, Jr., *J. Amer. Chem. Soc.*, **96**, 3327 (1974).
(20) J. G. Norman, Jr., and H. J. Kolari, *J. Chem. Soc., Chem. Commun.*, 303 (1974).
(21) J. V. Brencic and F. A. Cotton, *Inorg. Chem.*, **9**, 351 (1970).
(22) R. P. Messmer, L. V. Interrante, and K. H. Johnson, *J. Amer. Chem. Soc.*, **96**, 3847 (1974).
(23) J. V. Brencic and F. A. Cotton, *Inorg. Chem.*, **9**, 346 (1970).
(24) K. Schwarz, *Phys. Rev. B.*, **5**, 2466 (1972).
(25) J. G. Norman, Jr., *J. Chem. Phys.*, in press.
(26) R. E. Watson, *Phys. Rev.*, **111**, 1108 (1958).
(27) H. B. Gray, personal communication.
(28) R. J. H. Clark, personal communication.
(29) F. A. Cotton and J. G. Norman, Jr., *J. Amer. Chem. Soc.*, **93**, 80 (1971).
(30) J. G. Norman, Jr., and H. J. Kolari, unpublished results.
(31) A. P. Mortola, J. W. Moskowitz, N. Rösch, C. D. Cowman, and H. B. Gray, *Chem. Phys. Lett.*, in press.
(32) NOTE ADDED IN PROOF: Consistently, Cl–Cl = 3.36 Å in $Mo_2Cl_8^{4-}$, *less* than the van der Waals contact distance of 3.6 Å.